HHS Public Access

Author manuscript

Hear Res. Author manuscript; available in PMC 2023 September 15.

Published in final edited form as:

Hear Res. 2022 September 15; 423: 108376. doi:10.1016/j.heares.2021.108376.

How much prestin motor activity is required for normal hearing?

Kazuaki Homma[a,b,*], **Satoe Takahashi**[a], **Mary Ann Cheatham**[b,c,*]

[a]Department of Otolaryngology – Head and Neck Surgery, Feinberg School of Medicine, Northwestern University, Chicago, IL 60611, USA

[b]The Hugh Knowles Center for Clinical and Basic Science in Hearing and Its Disorders

[c]Department of Communication Sciences and Disorders, Northwestern University, Evanston, IL 60208, USA

Abstract

Prestin (SLC26A5) is a membrane-based voltage-dependent motor protein responsible for outer hair cell (OHC) somatic electromotility. Its importance for mammalian cochlear amplification has been demonstrated using mouse models lacking prestin (prestin-KO) and expressing dysfunctional prestin, prestin$^{V499G/Y501H}$ (499-prestin-KI). However, it is still not elucidated how prestin contributes to the mechanical amplification process in the cochlea. In this study, we characterized several prestin mouse models in which prestin activity in OHCs was variously manipulated. We found that near-normal cochlear function can be maintained even when prestin activity is significantly reduced, suggesting that the relationship between OHC electromotility and the peripheral sensitivity to sound may not be linear. This result is counterintuitive given the large threshold shifts in prestin-KO and 499-prestin-KI mice, as reported in previous studies. To reconcile these apparently opposing observations, we entertain a voltage- and turgor pressure-based cochlear amplification mechanism that requires prestin but is insensitive to significant reductions in prestin protein expression.

Keywords

SLC26A5; prestin; cochlear amplification; outer hair cells; electromotility

1. INTRODUCTION

Prestin (SLC26A5) is the voltage-operated membrane-based molecular motor (Zheng, et al., 2000) that confers somatic electromotility (Brownell, et al., 1985) on cochlear outer hair cells (OHCs). Previous studies found that mouse models lacking prestin (*Slc26a*$^{-/-}$, prestin-

*Address correspondence to: Kazuaki Homma (k-homma@northwestern.edu) and Mary Ann Cheatham (m-cheatham@northwestern.edu).

Declaration of competing interest

The authors declare no competing financial interests or conflicts of interest.

KO) suffer approximately 50 dB threshold shifts across frequency (Cheatham, et al., 2004; Liberman, et al., 2002; Wu, et al., 2004). Although these studies established the importance of prestin for mammalian cochlear amplification, how prestin-driven OHC electromotility contributes to the amplification process remains unclear, given that the absence of prestin resulted in significant morphological (shorter OHC length) and mechanical (reduced OHC axial stiffness) changes (Dallos, et al., 2008; Liberman, et al., 2002). To circumvent these issues, a knockin (KI) mouse model expressing prestin with triple mutations, prestin$^{K233Q/K235Q/R236Q}$ (abbreviated as C1-prestin), was generated. Despite its largely shifted voltage operating point (V_{pk}) in the hyperpolarizing direction (Oliver, et al., 2001), C1-prestin-KI mice did not show threshold shifts (Gao, et al., 2007). Later, another KI mouse model expressing prestin with V499G and Y501H double mutations (abbreviated as 499-prestin) was also generated (Dallos, et al., 2008). 499-prestin is virtually nonfunctional within the physiological voltage range, but it targets the cell membrane normally and confers wildtype (WT)-like OHC morphology and axial stiffness (Dallos, et al., 2008; Homma, et al., 2013; Zheng, et al., 2005). This 499-prestin-KI mouse model showed prestin-KO-like threshold shifts across frequency, thereby providing the first compelling experimental evidence that prestin-based OHC electromotility is indeed essential for normal cochlear amplification in mammals (Dallos, et al., 2008). The importance of prestin-mediated OHC electromotility for normal cochlear function was also demonstrated using prestin chimeric mice that showed a proportional decrease in sensitivity as the number of OHCs lacking prestin increased (Cheatham, et al., 2009).

The contribution of prestin to cochlear amplification was further investigated using prestin hypomorphic mice that express significantly reduced amounts of prestin (30–50% as compared to WT controls) in each OHC (Yamashita, et al., 2012). As predicted, the reduced prestin expression resulted in reductions of OHC length and electromotility. Surprisingly, however, ABR thresholds in hypomorphic mice were found to be WT-like for stimuli processed in the apical 2/3 of the cochlea (Yamashita, et al., 2012). It is also emphasized that the retention of WT-like sensitivity found in C1-prestin-KI mice was originally explained based on the then generally presumed resting membrane potential of OHCs, i.e., −70 mV, at which the magnitudes of electromotility were comparable in WT- and C1-prestin-expressing OHCs (Gao, et al., 2007). However, this explanation is no longer tenable considering the subsequent finding that OHC resting membrane potentials are depolarized to about −40 mV under physiological conditions where the apical surfaces of OHCs are exposed to endolymph containing high K^+ and low Ca^{2+} (Johnson, et al., 2011).

In summary, prestin-KO, 499-prestin-KI, and prestin chimeric mice demonstrate the importance of prestin-mediated OHC electromotility for normal cochlear function, whereas prestin hypomorphic and C1-prestin-KI mice provide seemingly opposing results. In the present study, we further investigated the contribution of prestin to cochlear amplification and found that hearing sensitivity can indeed be insensitive to large reductions of prestin-mediated motor activity. In the discussion, we propose a voltage- and turgor pressure-based mechanism that can sustain adequate levels of amplification even when prestin protein expression is reduced relative to WT.

2. Materials and methods

2.1 Animals

Care and use of the animals in this study were approved by the National Institutes of Health and the Animal Care and Use Committee at Northwestern University. C1-prestin-KI, 499-prestin-KI, and prestin-KO mice were generated and described in detail in previous studies (Dallos, et al., 2008; Gao, et al., 2007; Liberman, et al., 2002). The heterozygous and compound heterozygous mice used in this study were generated by crossing these various mouse models. All of the mice used in this study were on a mixed 129S/C57BL6 background. Except for one *Slc26a5*$^{C1/C1}$ who was 3 months old, all other subjects were less than 2 months of age (postnatal days 18–47).

2.2 *In vivo* electrophysiology

Gross cochlear potentials were acquired at the round window membrane using a silver-wire ball electrode in adolescent mice anesthetized with sodium pentobarbital (80 mg/kg ip). Rectal temperature was maintained at 38 °C, and the head holder was heated to minimize cooling of the cochlea. Responses were band-pass filtered (0.2–3.0 kHz) and a 10 μV N1/P1 criterion voltage designated compound action potential (CAP) threshold. Further details are provided in a previous publication (Cheatham, et al., 2004). Because distortion product otoacoustic emissions (DPOAEs) are associated with OHC function, these measures were also recorded using EmAv software (Neely and Liu, 1994) to evaluate changes in *Slc26a5*$^{499/+}$, *Slc26a5*$^{C1/C1}$, *Slc26a5*$^{C1/-}$, and *Slc26a5*$^{C1/499}$ mice anesthetized with ketamine (100 mg/kg ip) and xylazine (10 mg/kg ip). For emission measurements, a two-tone input was used with a frequency ratio of 1.2. A custom emission probe was inserted into the ear canal to form a tight seal allowing calibrations to be performed in each individual subject using SysRes (Neely and Stevenson, 1992) and a Card Deluxe 24-bit sound card with a sampling rate of 96 kHz. Data in this report are provided as iso-input functions where $L_1 = L_2 = 70$ dB SPL and as input-output or growth functions collected for $f_2 = 12$ kHz and when the level of f_1 (L_1) was 10 dB SPL greater than the level of f_2 (L_2). Additional details are provided in a previous publication (Cheatham, et al., 2014).

2.3 Hair cell preparation and *in vitro* electrophysiology

In the majority of cases, *in vitro* electrophysiology was performed on the same mice used for the *in vivo* physiology. Following euthanasia (Euthasol, 200 mg/kg), OHCs were isolated as described previously (Homma, et al., 2013). Whole-cell recordings were performed at room temperature using the Axopatch 200B amplifier (Molecular Devices, Sunnyvale, CA). Recording pipettes were pulled from borosilicate glass to achieve initial bath resistances averaging 3–4 MΩ. For nonlinear capacitance (NLC) measurements, recording pipettes were filled with an intracellular solution containing (mM): 140 CsCl, 2 $MgCl_2$, 10 EGTA, and 10 HEPES (pH 7.3, 307 mOsmol/kg). Isolated OHCs were bathed in an extracellular solution containing (mM): 120 NaCl, 20 TEA-Cl, 2 $CoCl_2$, 2 $MgCl_2$, 10 HEPES (pH 7.3). Osmolality was adjusted to 309 mOsmol/kg with glucose. NLC was measured using a sinusoidal voltage stimulus (2.5 Hz, 120 or 150 mV amplitude) superimposed with two higher frequency stimuli (391 (f_1) and 781 (f_2) Hz, 10 mV amplitude) (Homma and Dallos, 2011). Current data were collected by jClamp (SciSoft Company, New Haven,

CT), and NLC determined using a fast Fourier transform-based admittance analysis (Santos-Sacchi, et al., 1998). For whole-cell membrane conductance recordings, isolated OHCs were bathed in an extracellular solution containing (mM): 142 NaCl, 4 KCl, 1.5 $CaCl_2$, 1 $MgCl_2$, 8 Na_2HPO_4, 2 NaH_2PO_4, and 10 glucose (pH 7.3). Osmolality of the bath solution was adjusted to 317 mOsmol/kg with glucose. Recording pipettes were filled with an intracellular solution containing (mM): 144 KCl, 2 $MgCl_2$, 8 Na_2HPO_4, 2 NaH_2PO_4, 10 glucose, 1 ATP, 0.1 GTP, and 0.5 EGTA (pH 7.3). Recordings were performed approximately one minute after establishing the whole-cell configuration to ensure complete intracellular dialysis with the pipette solution. Steady-state currents at various holding potentials (from −160 mV to +120 mV, 20 mV step) were determined and plotted against the Rs-corrected holding potentials to obtain IV curves. The resting membrane potentials were determined by current-clamp at 0 nA. While recording, the intracellular pressure was not adjusted, i.e., the pressure reading at the back of the recording pipette was 0 mmHg with respect to the atmospheric pressure. Because capillary force is unlikely to be identical among recording pipettes, and because the osmolality of the bath solution slowly changes over time due to evaporation, there may have been slight variations in turgor between recordings.

2.4 NLC data analysis

NLC (C_m) data were analyzed using the following equation:

$$C_m = \frac{\alpha Q_{max} exp\left[\alpha\left(V_m - V_{pk}\right)\right]}{\left\{1 + exp\left[\alpha\left(V_m - V_{pk}\right)\right]\right\}^2} + C_{lin}$$

where α is the slope factor, Q_{max} is the maximum charge transfer, V_m is the membrane potential, V_{pk} is the voltage at which the maximum charge movement is attained, and C_{lin} is the linear capacitance.

2.5 Statistical analyses

Statistical analyses were performed using Prism (GraphPad Software). The Student's t-test was used for comparisons between two groups. One-way ANOVA combined with the Dunnett's post hoc test was used for multiple comparisons. In all statistical analyses, $p < 0.05$ was considered significant.

3. Results

3.1 *Slc26a5*$^{499/+}$ heterozygous mice

Disruption of one *Slc26a5* allele (*Slc26a5*$^{+/-}$) reduces prestin gene expression in OHCs. However, the amount of prestin protein produced by the remaining allele is much greater than 50% as compared to WT (*Slc26a5*$^{+/+}$) due to partial autoregulation (Cheatham, et al., 2005). Although prestin mRNA remains at approximately 50% of WT, prestin protein expression and OHC length are WT-like (Cheatham, et al., 2005). We, therefore, studied mice heterozygous for 499-prestin (*Slc26a5*$^{499/+}$) (Zheng, et al., 2005) to determine the effect of reducing prestin protein expression. 499-prestin targets the cell membrane

normally and confers WT-like cell morphology and axial stiffness on OHCs but is virtually nonfunctional within the physiological voltage range due to its extremely shifted V_{pk} in the depolarizing direction by approximately 250 mV (Dallos, et al., 2008; Homma, et al., 2013). In *Slc26a5*$^{499/+}$, both WT- and 499-prestin-expressing alleles contribute equally to produce comparable amounts of WT- and 499-prestin proteins, resulting in significantly reduced NLC and electromotility without changing OHC length (Homma, et al., 2013). Despite this large reduction in prestin activity, thresholds for compound action potentials (CAP) in young, early generation 499-prestin heterozygous mice (red) are WT-like (Fig. 1A). Because otoacoustic emissions are associated with OHC function, DPOAEs were also examined and shown to be WT-like. The iso-input functions, obtained for $L_1 = L_2 = 70$ dB SPL in *Slc26a5*$^{499/+}$ heterozygotes (red), are comparable to the average control data (black) (Fig. 1B). In addition, DPOAE input-output functions for $f_2 = 12$ kHz were also collected (Fig. 1C). If one designates threshold as the level of f_1 generating a DPOAE of 0 dB SPL, then the mice with one copy of WT prestin and one copy of 499-prestin have thresholds similar to those of the controls.

3.2 *Slc26a5*$^{C1/-}$ and *Slc26a5*$^{C1/499}$ compound heterozygous mice

The C1 triple mutations, K233Q/K235Q/R236Q, result in a large hyperpolarizing shift of the voltage operating point (V_{pk}) of prestin (Gao, et al., 2007; Oliver, et al., 2001). It is probable that this hyperpolarizing V_{pk} shift is due to neutralization of the three positively charged residues located at the extracellular surface of the cell membrane, which depolarizes the true transmembrane electric potential (Kuwabara, et al., 2018). This large hyperpolarizing V_{pk} shift should make the voltage-induced mechanical response of prestin at the physiological resting membrane potential of OHCs, i.e., around −40 mV (Johnson, et al., 2011), significantly smaller as compared to WT. However, C1-prestin-KI mice show WT-like sensitivity assayed using CAP thresholds (Gao, et al., 2007).

In order to further reduce prestin activity, we crossed C1-prestin-KI mice with prestin-KO and with 499-prestin-KI mice to obtain *Slc26a5*$^{C1/-}$ and *Slc26a5*$^{C1/499}$, respectively. Data in Fig. 2 indicate that both α and V_{pk} are reduced in *Slc26a5*$^{C1/C1}$, *Slc26a5*$^{C1/-}$, and *Slc26a5*$^{C1/499}$ mice. For *Slc26a5*$^{C1/C1}$, both Q_{max} and C_{lin} were statistically indistinguishable from those of WT, but their means were slightly larger and smaller than WT, respectively, which resulted in increased charge density with statistical significance. As predicted, the expression of C1-prestin was significantly reduced in both *Slc26a5*$^{C1/-}$ and *Slc26a5*$^{C1/499}$ but to a greater degree in *Slc26a5*$^{C1/499}$, as indicated by its smaller Q_{max}. Because charge density is adjusted for cell length, the reduced linear capacitance in *Slc26a5*$^{C1/-}$ OHCs is taken into account when using this metric. The shorter OHCs in *Slc26a5*$^{C1/-}$ mice are likely due to reduced levels of C1-prestin protein. Although some autoregulation may occur, it is not sufficient to produce WT-like OHC lengths.

We also performed another set of whole-cell recordings to explore the possibility that the expression of C1- or 499-prestin might increase the excitability of OHCs, as previous studies reported functional interaction between prestin and Kv7.4 (Chambard and Ashmore, 2005; Perez-Flores, et al., 2020). We found that the current-voltage relationships (Figs. 3A and 3B)

and the resting membrane electric potentials (Fig. 3C) of OHCs isolated from *Slc26a5*$^{C1/C1}$ and *Slc26a5*$^{499/499}$ did not show signs of increased OHC excitability as compared to WT.

Figure 4 provides DPOAE iso-input functions obtained at 70 dB SPL for *Slc26a5*$^{C1/C1}$, *Slc26a5*$^{C1/-}$, and for *Slc26a5*$^{C1/499}$ in the top panel and input-output functions at f_2 = 12 kHz in the bottom panel. Consistent with the reported WT-like CAP thresholds in *Slc26a5*$^{C1/C1}$ (Gao, et al., 2007), the DPOAEs are near-normal in mice with triple C1 mutations (blue). Similar results were obtained for the *Slc26a5*$^{C1/-}$ (green) and *Slc26a5*$^{C1/499}$ (magenta) mice, except that there were statistically significant magnitude reductions at high and low f_2 frequencies that may relate to reductions in C1 protein expression. However, given the large reduction in prestin activity (Fig. 2), these changes are surprisingly small. Taken together, these observations suggest that OHC function can be kept at near-normal levels despite significant reductions in prestin activity.

4. Discussion

OHC electromotility driven by prestin's voltage-dependent motor activity is demonstrated to be essential for normal cochlear amplification (Dallos, et al., 2008). In fact, a positive correlation between the threshold elevations vs. the numbers of prestin-deficient OHCs was found in a chimeric mouse model in which the ratio of prestin-deficient OHCs to WT OHCs varied among individual chimeric mice (Cheatham, et al., 2009). In this chimeric model, normal thresholds were not observed for low prestin-deficient OHC ratios (see Fig. 9 in Cheatham et al., 2009). Another study found significant threshold elevations in α-tectorin^{C1509G} mice in which the tectorial membrane (TM) attaches to OHCs only in the first row in heterozygotes and to no OHCs in homozygotes due to malformation of the TM caused by the p.C1509G missense mutation in α-tectorin (Xia, et al., 2010). Interestingly, upregulation of prestin was found in this mouse model, implying compensation for reduced numbers of TM-coupled OHCs (Xia, et al., 2010). However, this upregulation in OHCs that remained connected to the TM did not result in sensitive ABR or DPOAE responses (see Fig. 6 in Xia et al., 2010). Collectively, these observations reaffirm the indispensability of prestin-based motor activity for normal cochlear amplification.

In the present study, we expected to find hearing defects in *Slc26a5*$^{499/+}$, *Slc26a5*$^{C1/-}$, and *Slc26a5*$^{C1/499}$ mice. However, these mice did not show large changes when compared with WT controls. Although surprising, our results agree with a study by Yamashita and colleagues (Yamashita, et al., 2012) that also examined the influence of reduced prestin activity on sensitivity using hypomorphic mouse models where prestin expression was vastly reduced by destabilizing prestin mRNA. They found that reduction of prestin expression by as much as 70% did not affect ABR thresholds for frequencies up to and including 22 kHz. OHC function assessed by DPOAE measurements was also found to be WT-like (Yamashita, et al., 2012).

Taken together, these observations suggest that mammalian cochlear amplification is sensitive to reduction in the number of prestin-expressing OHCs but not to significant decreases in prestin protein. How might this be achieved?

Prestin is the major contributor to the global axial stiffness of OHCs. Elimination or inhibition (removal of intracellular chloride) of prestin is known to drastically reduce OHC axial stiffness (Dallos, et al., 2008; He, et al., 2003). This prestin-associated stiffness was demonstrated to be voltage-dependent (He and Dallos, 1999; He, et al., 2003), although an opposing report exists (Hallworth, 2007). Theoretically, this voltage-dependent stiffness change can cause OHC length changes if the cell is mechanically preloaded (Dallos and He, 2000). Fig. 5A shows the prestin-associated voltage-dependent axial stiffness of OHCs expressing WT- or C1/499-prestin, as deduced from their NLC parameters (Fig. 2). It is tempting to entertain the possibility that OHC electromotility (Δd) is primarily powered by OHC turgor pressure (P) and voltage-dependent axial stiffness changes (Δk_v), i.e., $\Delta d = P / \Delta k_v$. The signature cylindrical shape of OHCs, where their lateral membranes are surrounded by perilymph and not physically in contact with other structures, is advantageous for this hypothetical turgor pressure-driven electromotility mechanism. In this model, the magnitude of electromotility is modulated by turgor pressure. In fact, it was demonstrated that increasing turgor pressure increases the magnitude of OHC electromotility (Kakehata and Santos-Sacchi, 1995; Sziklai and Dallos, 1997) (but not in (Adachi, et al., 2000)). It has also been shown that perfusion of hypotonic perilymph, which is expected to increase turgor pressure, enhances cochlear amplification in anesthetized animals (Choi and Oghalai, 2008). In addition to its role as a competitor to the required chloride binding site, the prestin inhibitor, salicylate, was reported to reduce OHC turgor (Shehata, et al., 1991), implying its dual roles in inhibiting cochlear amplification. It is conceivable that OHC turgor pressure is actively regulated, and that it is higher in *Slc26a5*$^{499/+}$, *Slc26a5*$^{C1/-}$, and *Slc26a5*$^{C1/499}$ to produce WT-like electromotility. Aside from its effect on the magnitude of electromotility, turgor pressure also affects V_{pk} (Adachi, et al., 2000; Kakehata and Santos-Sacchi, 1995). Specifically, V_{pk} shifts in the depolarizing direction in response to increased turgor pressure. This behavior should facilitate the action of C1-prestin so that it works effectively within the physiological voltage range. It should be noted that prestin-associated OHC axial stiffness can be insensitive to the amount of the prestin protein. As shown in Fig. 5B, the overall stiffness (k_{all}) is proportional to the number of unitary stiffness (k) components connected in parallel but inversely proportional to those connected in series. This relationship suggests that a large augmentation in OHC turgor pressure would not be needed to compensate for reductions in prestin expression/activity.

SLC26A5 is an established deafness gene (DFNB61) abundantly expressed in OHCs. Although functional expression of prestin in cardiomyocytes was reported recently (Zhang, et al., 2021), prestin-KO mice are fully viable and able to reproduce. Nevertheless, only a few prestin variants have been identified in human patients, which is in stark contrast to over six hundred deafness-associated variants found in another deafness-associated SLC26 gene, pendrin (*SLC26A4*) (Stenson, et al., 2017). The small number of *SLC26A5* variants may not be surprising given the high tolerance of cochlear function to large reductions of prestin activity. Hence, it is crucial to determine the prestin activity that is minimally needed to sustain normal cochlear amplification in order to define the exact physiological role of prestin and, thus, to determine the pathogenicity of prestin variants.

Acknowledgements

This work was supported by NIH grants DC017482 (to KH), DC00089 (to MAC), and by the Hugh Knowles Center.

Abbreviations:

CAP	compound action potential
DPOAE	distortion product otoacoustic emission
OHC	outer hair cell
NLC	nonlinear capacitance
C1-prestin	prestin$^{K233Q/K235Q/R236Q}$
499-prestin	prestin$^{V499G/Y501H}$
WT	wildtype
KI	knockin
KO	knockout

References

Adachi M, Sugawara M, and Iwasa KH, 2000. Effect of turgor pressure on outer hair cell motility. J Acoust Soc Am 108(5 Pt 1), 2299–2306. 10.1121/1.1314396. [PubMed: 11108370]

Brownell WE, Bader CR, Bertrand D, and de Ribaupierre Y, 1985. Evoked mechanical responses of isolated cochlear outer hair cells. Science 227(4683), 194–196. 10.1126/science.3966153. [PubMed: 3966153]

Chambard JM, and Ashmore JF, 2005. Regulation of the voltage-gated potassium channel KCNQ4 in the auditory pathway. Pflugers Arch 450(1), 34–44. 10.1007/s00424-004-1366-2. [PubMed: 15660259]

Cheatham MA, Goodyear RJ, Homma K, Legan PK, Korchagina J, Naskar S, Siegel JH, Dallos P, Zheng J, and Richardson GP, 2014. Loss of the tectorial membrane protein CEACAM16 enhances spontaneous, stimulus-frequency, and transiently evoked otoacoustic emissions. J Neurosci 34(31), 10325–10338. 10.1523/JNEUROSCI.1256-14.2014. [PubMed: 25080593]

Cheatham MA, Huynh KH, Gao J, Zuo J, and Dallos P, 2004. Cochlear function in Prestin knockout mice. J Physiol 560(Pt 3), 821–830. 10.1113/jphysiol.2004.069559. [PubMed: 15319415]

Cheatham MA, Low-Zeddies S, Naik K, Edge R, Zheng J, Anderson CT, and Dallos P, 2009. A chimera analysis of prestin knock-out mice. J Neurosci 29(38), 12000–12008. 10.1523/JNEUROSCI.1651-09.2009. [PubMed: 19776286]

Cheatham MA, Zheng J, Huynh KH, Du GG, Gao J, Zuo J, Navarrete E, and Dallos P, 2005. Cochlear function in mice with only one copy of the prestin gene. J Physiol 569(Pt 1), 229–241. 10.1113/jphysiol.2005.093518. [PubMed: 16166160]

Choi CH, and Oghalai JS, 2008. Perilymph osmolality modulates cochlear function. Laryngoscope 118(9), 1621–1629. 10.1097/MLG.0b013e3181788d72. [PubMed: 18607303]

Dallos P, and He DZ, 2000. Two models of outer hair cell stiffness and motility. J Assoc Res Otolaryngol 1(4), 283–291. 10.1007/s101620010048. [PubMed: 11547808]

Dallos P, Wu X, Cheatham MA, Gao J, Zheng J, Anderson CT, Jia S, Wang X, Cheng WH, Sengupta S, et al. , 2008. Prestin-based outer hair cell motility is necessary for mammalian cochlear amplification. Neuron 58(3), 333–339. 10.1016/j.neuron.2008.02.028. [PubMed: 18466744]

Gao J, Wang X, Wu X, Aguiñaga S, Huynh K, Jia S, Matsuda K, Patel M, Zheng J, Cheatham M, et al. , 2007. Prestin-based outer hair cell electromotility in knockin mice does not appear to adjust the operating point of a cilia-based amplifier. Proc Natl Acad Sci U S A 104(30), 12542–12547. 10.1073/pnas.0700356104. [PubMed: 17640919]

Hallworth R, 2007. Absence of voltage-dependent compliance in high-frequency cochlear outer hair cells. J Assoc Res Otolaryngol 8(4), 464–473. 10.1007/s10162-007-0097-4. [PubMed: 17934775]

He DZ, and Dallos P, 1999. Somatic stiffness of cochlear outer hair cells is voltage-dependent. Proc Natl Acad Sci U S A 96(14), 8223–8228. 10.1073/pnas.96.14.8223. [PubMed: 10393976]

He DZ, Jia S, and Dallos P, 2003. Prestin and the dynamic stiffness of cochlear outer hair cells. J Neurosci 23(27), 9089–9096. [PubMed: 14534242]

Homma K, and Dallos P, 2011. Evidence that prestin has at least two voltage-dependent steps. J Biol Chem 286(3), 2297–2307. 10.1074/jbc.M110.185694. [PubMed: 21071769]

Homma K, Duan C, Zheng J, Cheatham MA, and Dallos P, 2013. The V499G/Y501H mutation impairs fast motor kinetics of prestin and has significance for defining functional independence of individual prestin subunits. J Biol Chem 288(4), 2452–2463. 10.1074/jbc.M112.411579. [PubMed: 23212912]

Johnson SL, Beurg M, Marcotti W, and Fettiplace R, 2011. Prestin-driven cochlear amplification is not limited by the outer hair cell membrane time constant. Neuron 70(6), 1143–1154. 10.1016/j.neuron.2011.04.024. [PubMed: 21689600]

Kakehata S, and Santos-Sacchi J, 1995. Membrane tension directly shifts voltage dependence of outer hair cell motility and associated gating charge. Biophys J 68(5), 2190–2197. 10.1016/S0006-3495(95)80401-7. [PubMed: 7612863]

Kuwabara MF, Wasano K, Takahashi S, Bodner J, Komori T, Uemura S, Zheng J, Shima T, and Homma K, 2018. The extracellular loop of pendrin and prestin modulates their voltage-sensing property. J Biol Chem 293(26), 9970–9980. 10.1074/jbc.RA118.001831. [PubMed: 29777056]

Liberman MC, Gao J, He DZ, Wu X, Jia S, and Zuo J, 2002. Prestin is required for electromotility of the outer hair cell and for the cochlear amplifier. Nature 419(6904), 300–304. 10.1038/nature01059. [PubMed: 12239568]

Neely ST, and Liu Z, 1994. EMAV: otoacoustic emission averager. Technical Memo No 17, Boy's Town National Research Hospital, Omaha NE. 10.13140/RG.2.1.3515.3767.

Neely ST, and Stevenson R, 1992. SysRes: System Response Acquisition. Tech Memo No. 1. Omaha NE: Boystown National Research Hospital, Omaha NE. 10.13140/RG.2.1.3187.6967.

Oliver D, He DZ, Klöcker N, Ludwig J, Schulte U, Waldegger S, Ruppersberg JP, Dallos P, and Fakler B, 2001. Intracellular anions as the voltage sensor of prestin, the outer hair cell motor protein. Science 292(5525), 2340–2343. 10.1126/science.1060939. [PubMed: 11423665]

Perez-Flores MC, Lee JH, Park S, Zhang XD, Sihn CR, Ledford HA, Wang W, Kim HJ, Timofeyev V, Yarov-Yarovoy V, et al. , 2020. Cooperativity of Kv7.4 channels confers ultrafast electromechanical sensitivity and emergent properties in cochlear outer hair cells. Sci Adv 6(15), eaba1104. 10.1126/sciadv.aba1104. [PubMed: 32285007]

Santos-Sacchi J, Kakehata S, and Takahashi S, 1998. Effects of membrane potential on the voltage dependence of motility-related charge in outer hair cells of the guinea-pig. J Physiol 510 (Pt 1), 225–235. 10.1111/j.1469-7793.1998.225bz.x. [PubMed: 9625879]

Shehata WE, Brownell WE, and Dieler R, 1991. Effects of salicylate on shape, electromotility and membrane characteristics of isolated outer hair cells from guinea pig cochlea. Acta Otolaryngol 111(4), 707–718. 10.3109/00016489109138403. [PubMed: 1950533]

Stenson PD, Mort M, Ball EV, Evans K, Hayden M, Heywood S, Hussain M, Phillips AD, and Cooper DN, 2017. The Human Gene Mutation Database: towards a comprehensive repository of inherited mutation data for medical research, genetic diagnosis and next-generation sequencing studies. Hum Genet 136(6), 665–677. 10.1007/s00439-017-1779-6. [PubMed: 28349240]

Sziklai I, and Dallos P, 1997. Hyposmotic swelling induces magnitude and gain change in the electromotile performance of isolated outer hair cells. Acta Otolaryngol 117(2), 222–225. 10.3109/00016489709117775. [PubMed: 9105454]

Wu X, Gao J, Guo Y, and Zuo J, 2004. Hearing threshold elevation precedes hair-cell loss in prestin knockout mice. Brain Res Mol Brain Res 126(1), 30–37. 10.1016/j.molbrainres.2004.03.020. [PubMed: 15207913]

Xia A, Gao SS, Yuan T, Osborn A, Bress A, Pfister M, Maricich SM, Pereira FA, and Oghalai JS, 2010. Deficient forward transduction and enhanced reverse transduction in the alpha tectorin C1509G human hearing loss mutation. Dis Model Mech 3(3–4), 209–223. 10.1242/dmm.004135. [PubMed: 20142329]

Yamashita T, Fang J, Gao J, Yu Y, Lagarde MM, and Zuo J, 2012. Normal hearing sensitivity at low-to-middle frequencies with 34% prestin-charge density. PLoS One 7(9), e45453. 10.1371/journal.pone.0045453. [PubMed: 23029017]

Zhang XD, Thai PN, Ren L, Perez Flores MC, Ledford HA, Park S, Lee JH, Sihn CR, Chang CW, Chen WC, et al. , 2021. Prestin amplifies cardiac motor functions. Cell Rep 35(5), 109097. 10.1016/j.celrep.2021.109097. [PubMed: 33951436]

Zheng J, Du GG, Matsuda K, Orem A, Aguiñaga S, Deák L, Navarrete E, Madison LD, and Dallos P, 2005. The C-terminus of prestin influences nonlinear capacitance and plasma membrane targeting. J Cell Sci 118(Pt 13), 2987–2996. 10.1242/jcs.02431. [PubMed: 15976456]

Zheng J, Shen W, He DZ, Long KB, Madison LD, and Dallos P, 2000. Prestin is the motor protein of cochlear outer hair cells. Nature 405(6783), 149–155. 10.1038/35012009. [PubMed: 10821263]

Highlights

- Prestin-based motor activity is required for normal cochlear amplification.
- Various prestin mutations were used to study outer hair cell electromotility.
- Prestin mouse models with reduced motility retain near-normal hearing.
- Cochlear amplification can tolerate reductions in prestin protein expression.
- A turgor-pressure based motility mechanism is proposed to explain this tolerance.

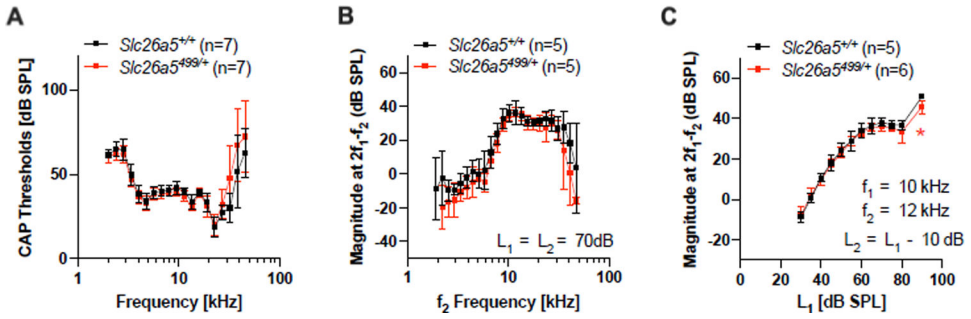

Fig. 1. CAPs and DPOAEs in *Slc26a5*$^{499/+}$ mice and their controls.

(**A**) CAP thresholds for *Slc26a5*$^{+/+}$ (WT) controls (postnatal days 28, 29, 30, 32, 33, 37, and 43) and for *Slc26a5*$^{499/+}$ heterozygous (postnatal days 28, 29, 29, 29, 31, 32, and 33) mice. (**B**) DPOAE iso-input functions for $2f_1$-f_2 obtained at $L_1 = L_2 = 70$ dB SPL. The ages of mice (postnatal days) were: 18, 18, 19, 19, and 21 for *Slc26a5*$^{+/+}$; 19, 19, 20, 21 and 21 for *Slc26a5*$^{499/+}$. (**C**) DPOAE input-output functions at $f_2 = 12$ kHz collected when the level of f_2 (L_2) was 10 dB SPL lower than the level of f_1 (L_1). Mouse ages (postnatal days) were: 18, 18, 19, 19, and 31 for *Slc26a5*$^{+/+}$; 18, 19, 19, 20, 21, and 21 for *Slc26a5*$^{499/+}$. In all panels, the results are provided as means and standard deviations. A statistically significant difference between *Slc26a5*$^{+/+}$ vs. *Slc26a5*$^{499/+}$ was found only in panel C at 90 dB SPL (denoted as *, $p = 0.01$) where the difference in the mean values was small.

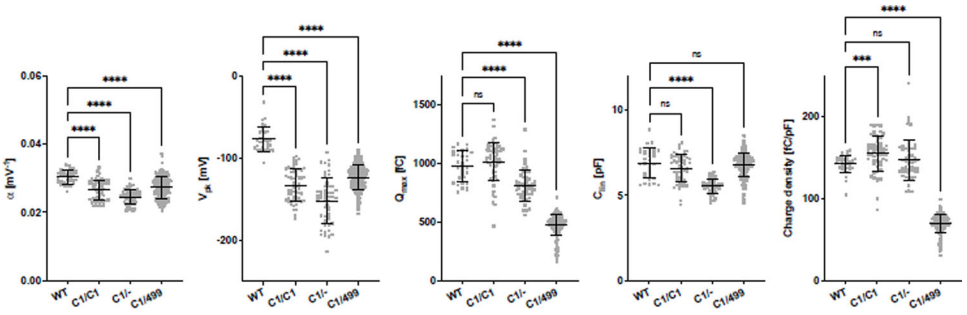

Fig. 2. NLC parameters of OHCs isolated from *Slc26a5*$^{+/+}$, *Slc26a5*$^{C1/C1}$, *Slc26a5*$^{C1/-}$, and *Slc26a5*$^{C1/499}$.

The α, V_{pk}, Q_{max}, C_{lin}, and charge density values [mean ± s.d. (n)] were as follows: WT [0.030 ± 0.002 mV^{-1}, −77 ± 15 mV, 979 ± 129 fC, 6.9 ± 0.9 pF, 143 ± 11 fC/pF (n=32)]; C1/C1 [0.027 ± 0.003 mV^{-1}, −133 ± 20 mV, 1017 ± 166 fC, 6.6 ± 0.8 pF, 155 ± 21 fC/pF (n=56)]; C1/− [0.025 ± 0.002 mV^{-1}, −152 ± 28 mV, 814 ± 131 fC, 5.5 ± 0.4 pF, 147 ± 25 fC/pF (n=50)]; C1/499 [0.027 ± 0.003 mV^{-1}, −124 ± 15 mV, 478 ± 88 fC, 6.8 ± 0.7 pF, 70 ± 11 fC/pF (n=200)]. Horizontal lines indicate means and standard deviations. ****, $p < 0.0001$. ***, $0.0001 < p < 0.001$. ns, $p > 0.05$. The ages of mice (postnatal days) were: 18, 24, 26, 27, 28, 29, 30, 31, 32, 33, and 44 for *Slc26a5*$^{+/+}$; 25, 27, 28, and 29 for *Slc26a5*$^{C1/C1}$; 22, 24, 25, and 31 for *Slc26a5*$^{C1/-}$; 22, 25, 26, 27, 28, 29, 30, 31, 34, 35, 37, and 43 for *Slc26a5*$^{C1/499}$.

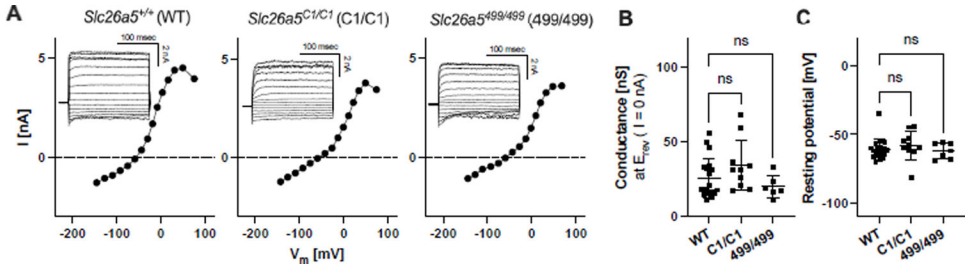

Fig. 3. Voltage-dependent membrane conductance of OHCs expressing WT-, C1-, or 499-prestin.

(**A**) Current-voltage (I-V) relationships determined for OHCs isolated from *Slc26a5*$^{+/+}$ (WT), *Slc26a5*$^{C1/C1}$ (C1/C1), and *Slc26a5*$^{499/499}$ (499/499) mice. Insets show current responses to rectangular command voltage steps from −160 mV to + 120 mV (20 mV step for 200 msec). V_m readings at 0 nA (broken horizontal lines) gave reversal potentials (E_{rev}). (**B**) A summary of the cell membrane conductance at E_{rev}. Horizontal bars indicate the mean ± SD: 26 ± 13 nS (n=19), 32 ± 17 nS (n=10), and 20 ± 8 nS (n=6) for WT, C1/C1, and 499/499, respectively. These values were statistically indistinguishable (one-way ANOVA followed by the Dunnett's Multiple Comparison Procedure). (**C**) The resting membrane potentials of OHCs determined by whole-cell current-clamp (at 0 nA). Horizontal bars indicate the mean ± SD: −61 ± 8 mV (n=19), −58 ± 11 mV (n=10), and −62 ± 5 mV (n=6) for WT, C1/C1, and 499/499, respectively. These values were statistically indistinguishable (one-way ANOVA followed by the Dunnett's Multiple Comparison Procedure). The ages of mice (postnatal days) were: 25, 33, and 34 for *Slc26a5*$^{+/+}$; 24, 25, 28, and 29 for *Slc26a5*$^{C1/C1}$; 32, 33, and 34 for *Slc26a5*$^{499/499}$.

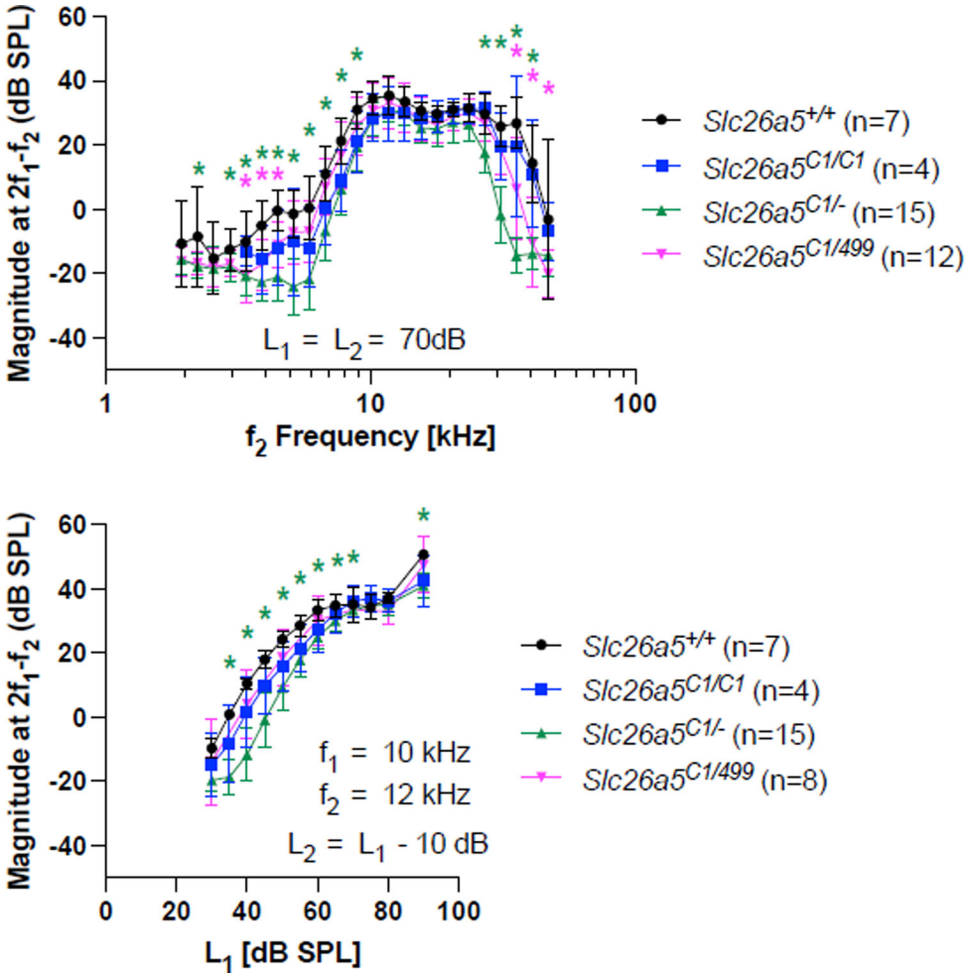

Fig. 4. DPOAEs in *Slc26a5*$^{C1/C1}$, *Slc26a5*$^{C1/-}$, and *Slc26a5*$^{C1/499}$ mice.

Iso-input functions collected at 70 dB SPL are provided in the top panel, input-output functions at f_2 = 12 kHz in the bottom panel. In both panels, data are provided for *Slc26a5*$^{C1/C1}$ homozygotes (blue), *Slc26a5*$^{C1/-}$ heterozygotes (green), *Slc26a5*$^{C1/499}$ compound heterozygotes (magenta), and controls (black). The results are provided as means and standard deviations. Asterisks indicate statistically significant difference, $p < 0.05$, compared to WT controls (determined by one-way ANOVA followed by the Dunnett's Multiple Comparison Procedure). In the upper panel, the ages of mice (postnatal days) were: 18, 18, 18, 19, 19, 20, and 21 for *Slc26a5*$^{+/+}$; 19, 19, 19, and 104 for *Slc26a5*$^{C1/C1}$; 20, 20, 20, 20, 20, 21, 21, 21, 22, 22, 22, 22, 22, 29, and 29 for *Slc26a5*$^{C1/-}$; 23, 25, 25, 26, 27, 28, 29, 30, 31, 34, 35 and 47 for *Slc26a5*$^{C1/499}$. In the bottom panel, the ages of mice (postnatal days) were: 18, 18, 19, 19, 20, 23, and 31 for *Slc26a5*$^{+/+}$; 19, 19, 19, and 104 for *Slc26a5*$^{C1/C1}$; 20, 20, 20, 20, 21, 21, 21, 21, 22, 22, 22, 22, 22, 29, and 29 for *Slc26a5*$^{C1/-}$; 25, 28, 29, 30, 30, 32, 32, and 36 for *Slc26a5*$^{C1/499}$.

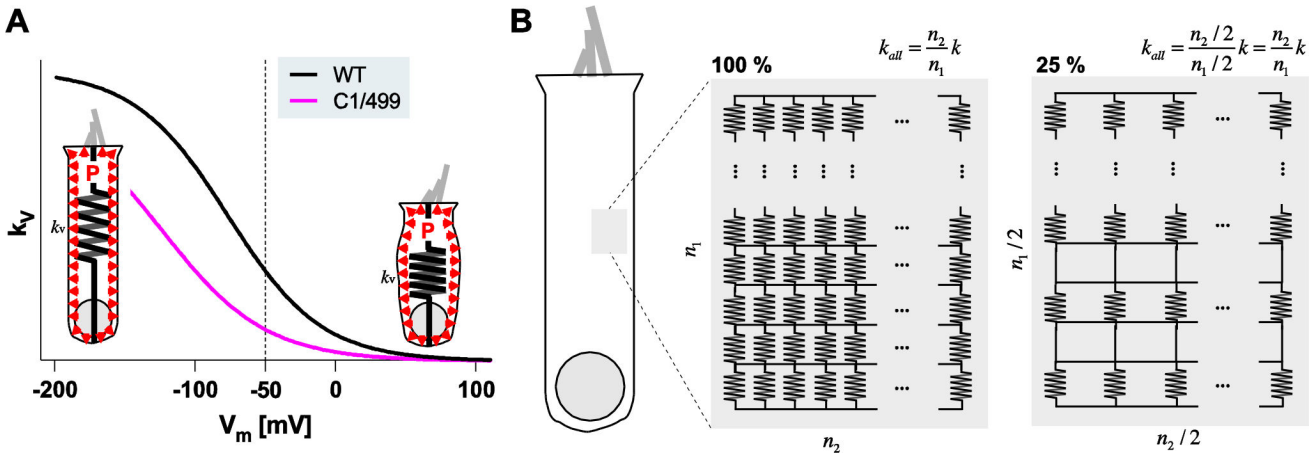

Fig. 5. A hypothetical electromotility mechanism driven by turgor pressure and voltage-dependent OHC axial stiffness.

(**A**) Voltage-dependent OHC axial stiffness, k_V, deduced from the NLC parameters of WT (black) and C1/499 compound heterozygotes (magenta). In this model, OHC electromotility is driven by turgor pressure, P (indicated by red arrow heads) and a prestin-associated voltage-dependent change in the axial stiffness (Δk_V). OHC contraction or elongation (Δd) is expressed as $\Delta d = P/\Delta k_V$. Circumferential inflation of an OHC due to positive turgor pressure with reduced axial stiffness is exaggerated for clarity. Note that this model is mathematically similar to the widely accepted prestin area motor-based electromotility mechanism ($F = k_V \times \Delta d$). (**B**) Schematic representations of the OHC lateral membrane with prestin-associated unitary voltage-dependent stiffness, k. n_1 and n_2 indicate the numbers of unitary stiffness components connected in series and in parallel, respectively. On the right, the total number of the unitary stiffness components is only 25% of those on the left, yet the overall stiffness, k_{all}, remains unchanged.